Precision Engineering 44 (2016) 252–256

Contents lists available at ScienceDirect

Precision Engineering

journal homepage: www.elsevier.com/locate/precision

Technical note

A new tunable dynamics platform for milling experiments

Tyler Ransom, Andrew Honeycutt, Tony Schmitz*

University of North Carolina at Charlotte, Charlotte, NC, United States

ARTICLE INFO

Article history:
Received 1 June 2015
Received in revised form
22 December 2015
Accepted 13 January 2016
Available online 25 January 2016

Keywords:
Machining
Dynamics
Chatter
Flexure
Eddy current damper

ABSTRACT

This paper describes a flexure-based platform with tunable dynamics that is used for milling stability experiments. Damping is added to a parallelogram, leaf-type flexure by incorporating an eddy current damper. Using this flexure/damper combination, the platform dynamics can be selected (tuned) at the design stage to match the desired experimental conditions. An increase in the dimensionless damping ratio of over 200% is demonstrated through the addition of the eddy current damper. The design analysis is detailed and experimental results are presented for modal testing and milling stability trials.

1. Introduction

Time and frequency domain milling process models may be implemented to enable pre-process parameter selection for increased material removal rate, improved surface finish, and enhanced accuracy (see [1–3], for example). To complete these simulations and validate the results, the system dynamics must be known. Typically, the cutting tool flexibility dominates the system dynamics, although the workpiece can introduce significant flexibility in some cases as well.

To realize a validation platform with simple (often single degree of freedom) dynamics, flexures may be used to support the workpiece (see Fig. 1). In this configuration, the flexure stiffness may be selected to be much lower than the tool stiffness so that the tool dynamics can be effectively ignored. One aspect of using flexures is that the damping is low (typically 1% or less). It may be desired, however, to perform milling experiments on a system with increased damping. In this paper, a flexure platform is described which offers an ideal setup for milling process dynamics experiments. It offers stiffness, natural frequency, and viscous damping values that can be tuned using first principles models at the design stage to match the desired frequency response. In this way, structural dynamics can be adjusted to test milling models over a broad range. An example application is machining of the monolithic thin-walled structures that are common in the aerospace industry [4–8].

2. Milling platform concept

The basis for the milling platform designed and tested in this study is a parallelogram, leaf-type flexure. By selecting the leaf geometry and workpiece/platform mass, the stiffness and natural frequency can be defined to meet the experimental requirements. The design approach is described in [9] and, for brevity, is not discussed here. As noted, however, the damping for this geometry, particularly monolithic designs, is low.

To introduce higher damping using a first principles model, the addition of an eddy current damper to the flexure setup is investigated here. The viscous (velocity-dependent) damping force for an eddy current damper can be described analytically. Fig. 2 displays the motion of a conductor[1] relative to a magnet (or magnet pair) with the motion perpendicular to the magnet pole direction. The eddy current density, $\vec{J}$, depends on the conductivity, σ, and the cross product of the velocity, $\vec{v}$, and magnetic field, $\vec{B}$ (see Eq. (1)). The eddy current force is then calculated as the volume integral of the product of the eddy current density and the magnetic field (see Eq. (2)). Mathematically, the two cross products yield a damping force which acts in the direction opposite to the velocity.

$$\vec{J} = \sigma(\vec{v} \times \vec{B}) \tag{1}$$

$$\vec{F} = \int_V (\vec{J} \times \vec{B}) dV \tag{2}$$

* Corresponding author. Tel.: +1 17046875086.
E-mail address: tony.schmitz@uncc.edu (T. Schmitz).

[1] The conductor is a conductive, non-magnetic material. Aluminum and copper are common choices.

http://dx.doi.org/10.1016/j.precisioneng.2016.01.005
0141-6359/

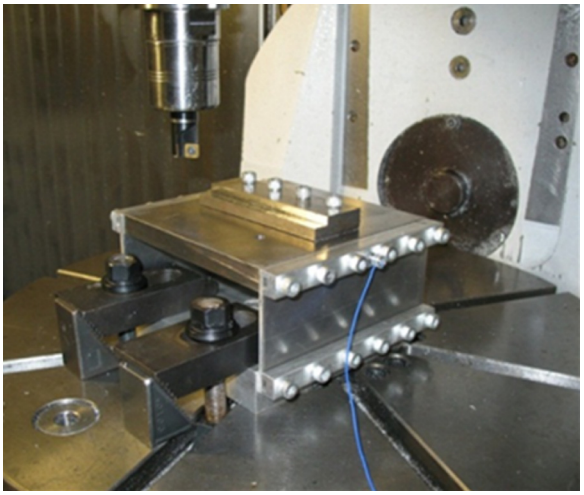

Fig. 1. Example parallelogram, leaf-type flexure used for milling experiments. A workpiece is mounted to the top of the flexure, an accelerometer is used to measure the vibration during cutting, and an inserted cutting tool is pictured.

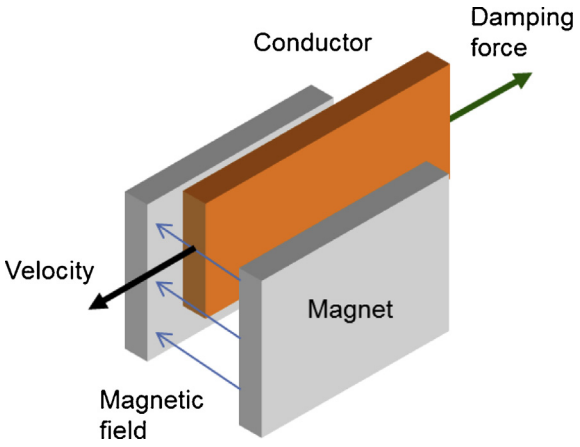

Fig. 2. Schematic of an eddy current damper.

The damping force magnitude, F, is described by Eq. (3), where δ is the conductor thickness, B is the magnetic field strength, S is the magnet surface area, α_1 incorporates surface charge effects, α_2 describes end effects from the finite dimension conductor, and v is the velocity magnitude [10]. The calculations for α_1 and α_2 are provided in Appendix A. As shown, Eq. (3) can be rewritten as the product of a viscous damping coefficient, c, and the velocity magnitude. This viscous damping coefficient enables model-based damping prediction and selection for milling simulation and experiments.

$$F = (\sigma\delta B^2 S(\alpha_1 + \alpha_2))v = cv \tag{3}$$

The eddy current damper concept displayed in Fig. 2 was embedded inside an aluminum flexure as shown in Fig. 3. The conductor was attached to the aluminum flexure platform and two permanent magnet sets were attached to the aluminum flexure base, one on each side of the conductor. The arrangement of the eight 25.4 mm square neodymium magnets (K&J Magnetics BXOXO8DCB) is shown in Fig. 4; aluminum socket head cap screws were used to avoid disrupting the magnetic field.

3. Damped flexure design

The solid model displayed in Fig. 3 was constructed and tested. As shown in Eq. (3), the viscous damping coefficient can

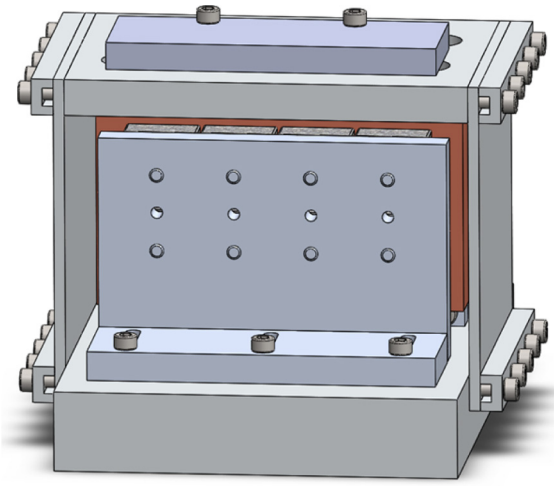

Fig. 3. Flexure with embedded eddy current damper.

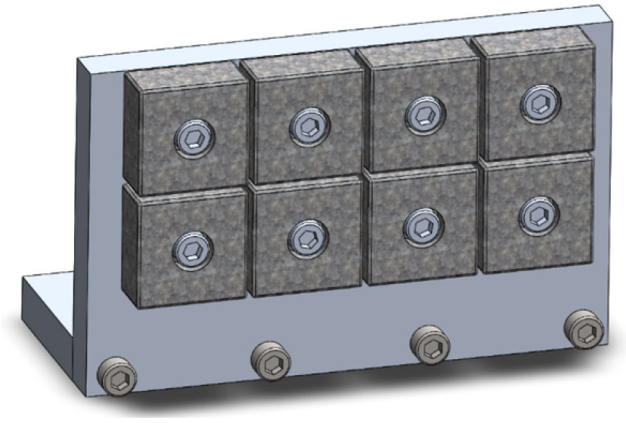

Fig. 4. Permanent magnet mount. The magnets face the conductor with one mount one each side.

Table 1
Eddy current damper design parameters.

Parameter	Value
σ	5.96×10^7 A/V m
δ	19.1 mm
B	4580 Gauss (0.458 T)
S	4.6×10^{-3} m^2
α_1[a]	0.352
α_2[a]	−0.177

[a] Calculations for these terms are provided in Appendix A.

be predicted using σ, δ, B, S, and the surface charge/end effect terms, which serve to reduce the damping value (see Table 1). The conductor was a 19.1 mm thick copper plate that extended outside the magnet surface area. The magnetic field strength was measured at 64 locations over the surface of the eight permanent magnets using a gaussmeter (Integrity Design & Research Corp., IDR-329-T). Measurements were performed at a distance of 0.8 mm from the surface; this was the approximate air gap between the magnets and conductor after assembly. The average value for all 64 measurements at the 0.8 mm distance is listed in Table 1.

For the values listed in Table 1, the predicted eddy current damper c value is 192 N s/m. The corresponding dimensionless damping ratio, ζ, is calculated using Eq. (4), where k is the flexure stiffness provided in Eq. (5) and m is the equivalent flexure mass given by Eq. (6) [4]. In Eq. (5), E is the aluminum leaf's elastic modulus (69 GPa), w is the width (101.6 mm), t is the thickness (3.8 mm),

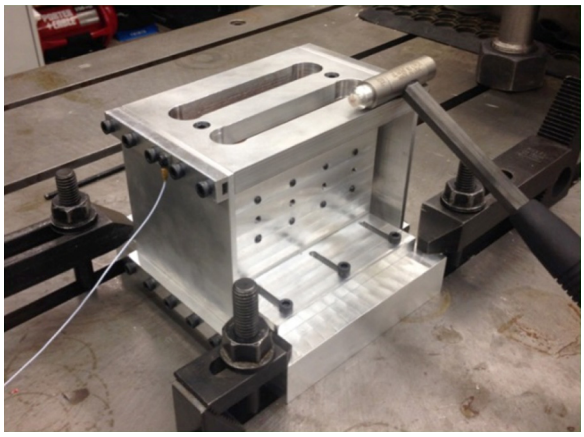

Fig. 5. Impact testing setup for experimental identification of damped flexure dynamics.

and l is the length (88.9 mm). In Eq. (6), m_p is the combined mass of the platform, conductor, top leaf clamps, and fasteners (2.098 kg) and m_l is the leaf mass (0.12 kg). The predicted damping ratio is 0.063 (6.3%). Using the flexure stiffness (1.093×10^6 N/m) and mass values (2.277 kg), the predicted undamped natural frequency is $f_n = 110$ Hz.

$$\zeta = \frac{c}{2\sqrt{km}} \tag{4}$$

$$k = 2 \quad Ew\left(\frac{t}{l}\right)^3 \tag{5}$$

$$m = m_p + \left(\frac{26}{35}\right) m_l \tag{6}$$

4. Experimental results

4.1. Modal testing

Modal tests were performed to identify the actual damping ratio for the flexure. The setup is shown in Fig. 5. An instrumented hammer (PCB 086C04) was used to excite the structure and the response was measured using a low-mass accelerometer (PCB 352C23). The modal parameters extracted from the single degree of freedom frequency response function were: $f_n = 110$ Hz, $k = 1.06 \times 10^6$ N/m, and $\zeta = 0.046$ (4.6%).[2] The disagreement in the damping ratio is attributed to approximations in the surface charge and end effects terms, α_1 and α_2. The eight individual magnets were assumed to comprise a single magnetic surface with the area reduced by the cap screw holes (see Appendix A). Also, the actual magnetic field strength is strongly sensitive to the air gap, which was set with a plastic shim during damper assembly, and the viscous damping coefficient varies with the square of this value.

Modal tests were also performed after removing the magnets so that the eddy current damping effect was eliminated, but the structure was not otherwise modified. The modal parameters extracted from the single degree of freedom frequency response function were: $f_n = 108$ Hz, $k = 9.03 \times 10^5$ N/m, and $\zeta = 0.014$. The addition of the eddy current damper provided a 229% increase in damping.

4.2. Machining trials

Given the successful fabrication and testing of the flexure, machining trials were completed to demonstrate: (1) agreement between the predicted and experimental milling stability as a function of spindle speed and axial depth of cut; and (2) the change in the stability behavior with and without the eddy current damper in place.

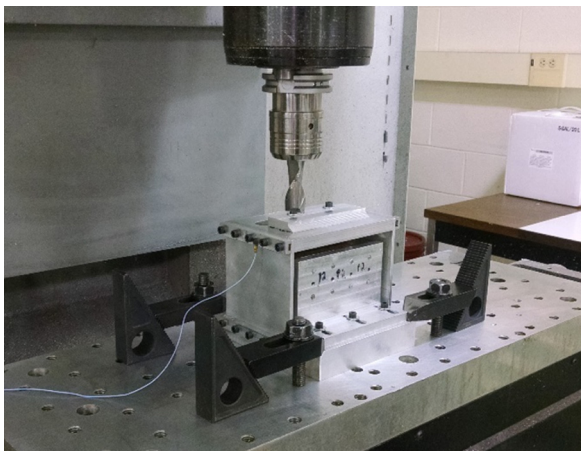

Fig. 6. Milling setup showing damped flexure, two-flute endmill, and accelerometer.

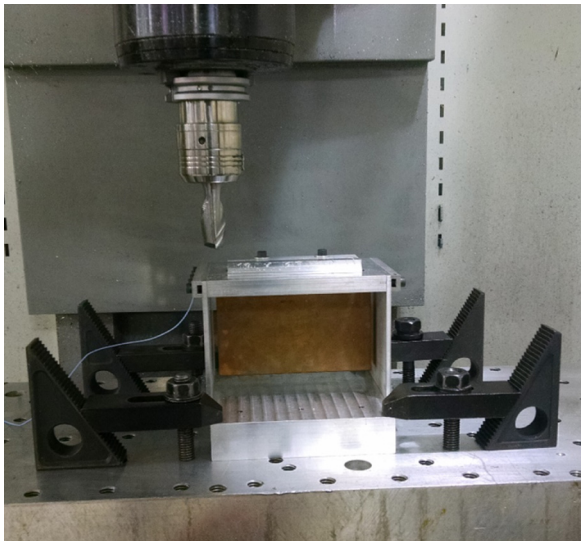

Fig. 7. Milling setup showing undamped flexure, two-flute endmill, and accelerometer.

A 6061-T6 workpiece was bolted to the platform top and modal tests were repeated for the new setup as mounted on the computer numerically controlled (CNC) milling machine (Haas TM-1) table (see Fig. 6), where the accelerometer attached to the flexure was used to identify stable and unstable cutting conditions. The new modal parameters were: $f_n = 110.6$ Hz, $k = 9.29 \times 10^5$ N/m, and $\zeta = 0.043$ with the magnets in place and: $f_n = 108$ Hz, $k = 9.03 \times 10^5$ N/m, and $\zeta = 0.015$ with no magnets. The setup with no magnets is displayed in Fig. 7. The percent difference in damping ratio is 187%. The change in damping performance is attributed to the change in air gap during assembly on the machine table.

For the two-flute endmill/6061-T6 aluminum workpiece, the specific cutting force was 700 N/mm^2 and the force angle was 70°. Using these values together with the flexure dynamics (the tool point frequency response was an order of magnitude stiffer and was ignored), stability lobe diagrams were generated using the average tooth angle approach for the damped and undamped flexure setups [1]. Figs. 8 and 9 show the limiting axial depth of cut (b_{lim}) as a function of spindle speed (Ω) for a 25% radial immersion

[2] The flexure was an order of magnitude stiffer in the orthogonal directions.

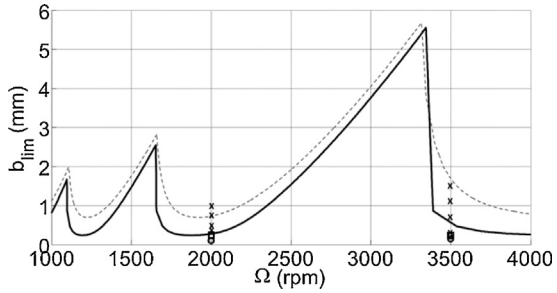

Fig. 8. Stability limit behavior for undamped flexure. The stability limits without magnets (solid) and with magnets (dashed) are shown for comparison. The undamped test points are identified as stable (circle), marginal (square), or unstable (cross). The results are also presented in Table 2.

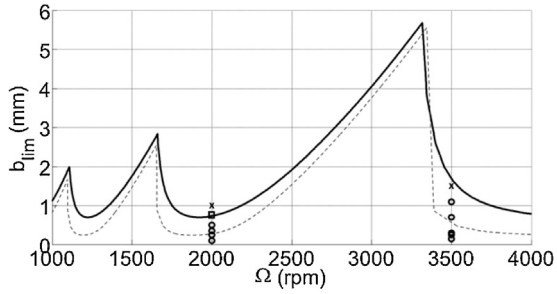

Fig. 9. Stability limit behavior for damped flexure. The stability limits with magnets (solid) and without magnets (dashed) are shown for comparison. The damped test points are identified as stable (circle), marginal (square), or unstable (cross). The results are also presented in Table 2.

up milling cut. Fig. 8 displays the test results for the undamped flexure, while Fig. 9 presents the damped flexure results.

As shown in Figs. 8 and 9, two spindle speeds were selected to validate the predicted milling stability behavior: 2000 rpm and 3500 rpm. In both cases, the predicted increase in the limiting depth of cut with the addition of the eddy current damper was obtained. The results are presented in Table 2. Cuts were identified as stable or unstable based on the frequency content of the accelerometer signal, A. If significant content amplitude was observed at frequencies other than the tooth passing frequency and its harmonics, the cut was considered unstable. The chatter frequency was verified to be near the flexure natural frequency in each case.

Representative accelerometer frequency content examples are provided for the undamped flexure at a spindle speed of 3500 rpm in Fig. 10 (0.15 mm axial depth) and Fig. 11 (0.7 mm). In Fig. 10, content at the tooth passing frequency (116.7 Hz) and its multiples (as well as the subharmonic runout frequencies) is observed. This cut is stable. In Fig. 11, on the other hand, the signal amplitude is 30 times larger with the dominant peak near the flexure natural frequency. This cut exhibited chatter.

Table 2
Stability testing results. *U* indicates the undamped flexure and *D* indicates the damped flexure. Stable = o, unstable = ×, marginal = m.

2000 rpm			3500 rpm		
b (mm)	*U*	*D*	*b* (mm)	*U*	*D*
0.1	o	o	0.15	o	o
0.25	m	o	0.25	m	o
0.35	×	o	0.3	×	o
0.5	×	o	0.7	×	o
0.75	×	m	1.1	×	o
1.0	×	×	1.5	×	×

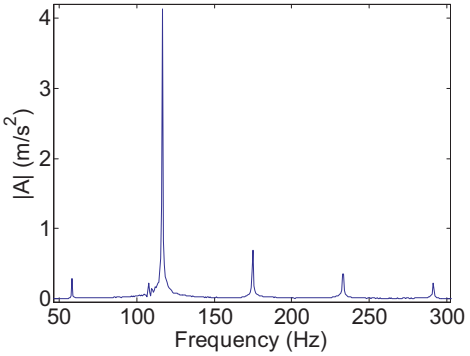

Fig. 10. Stable cut at 0.15 mm axial depth and 3500 rpm spindle speed for the undamped flexure.

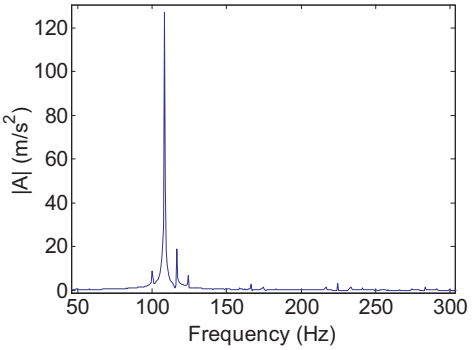

Fig. 11. Unstable cut at 0.7 mm axial depth and 3500 rpm spindle speed for the undamped flexure.

5. Conclusions

This study described a new approach for prescribing the structural dynamics in machining stability testing. It demonstrated a flexure-based platform with dynamics that can be selected at the design stage. Damping was added by introducing an eddy current damper into a traditional parallelogram, leaf-type flexure. The dimensionless damping ratio was increased by 229% with the addition of the eddy current damper. The design process was detailed so that other researchers can implement the new strategy.

Appendix A.

Modification of the viscous damping coefficient for the eddy current damper to account for surface charge effects and end effects is detailed in [10]. The final expressions are presented here for completeness.

The surface charge effects term, α_1, is calculated using Eq. (A1), where $2a$ is the height of the magnet area and $2b$ is the width. For the setup described here, $a = 25.4$ mm and $b = 50.8$ mm so that $\alpha_1 = 0.352$.

$$\alpha_1 = 1 - \frac{1}{2\pi}\left[4 \tan^{-1}\left(\frac{b}{a}\right) + \frac{b}{a}\ln\left(1+\frac{a^2}{b^2}\right) - \frac{a}{b}\ln\left(1+\frac{b^2}{a^2}\right)\right] \tag{A1}$$

The end effects term for the conductor, α_2, is determined using Eq. (A2), where I_1 and I_2 are defined by Eqs. (A3) and (A4). In these equations, $2H$ is the height of the conductor, $h = ba^{-1}$, and

$w = Ha^{-1}$. For the eddy current damper designed and constructed in this study, $H = 38.1$ mm and $\alpha_2 = -0.177$.

$$\alpha_2 = -\frac{1}{2\pi}(I_1 + I_2) \tag{A2}$$

$$I_1 = 4w \tan^{-1}\left(\frac{h}{w}\right) - 4(1-w)\tan^{-1}\left(\frac{h}{1-w}\right) + \frac{w^2}{h}\ln(w^2) - \frac{1}{h}(w^2-h^2)\ln(w^2+h^2) - \frac{1}{h}(1-w)^2\ln(1-w)^2 + \frac{1}{h}((1-w)^2-h^2)\ln((1-w)^2+h^2) \tag{A3}$$

$$I_2 = 4w\tan^{-1}\left(\frac{h}{w}\right) - 4(1+w)\tan^{-1}\left(\frac{h}{1+w}\right) + \frac{w^2}{h}\ln(w^2) - \frac{1}{h}(w^2-h^2)\ln(w^2+h^2) - \frac{1}{h}(1+w)^2\ln(1+w)^2 + \frac{1}{h}((1+w)^2-h^2)\ln((1+w)^2+h^2) \tag{A4}$$

References

[1] Schmitz T, Smith S. Machining dynamics: frequency response to improved productivity. New York, NY: Springer; 2009.
[2] Altintas Y. Manufacturing automation: metal cutting mechanics, machine tool vibrations, and CNC design. 2nd ed. New York, NY: Cambridge University Press; 2012.
[3] Altintas Y, Weck M. Chatter stability of metal cutting and grinding. CIRP Ann: Manuf Technol 2004;53(2):619–42.
[4] Tlusty J, Smith S, Winfough WR. Techniques for the use of long slender end mills in high-speed milling. CIRP Ann: Manuf Technol 1996;45(1):393–6.
[5] Smith S, Winfough WR, Halley J. The effect of tool length on stable metal removal rate in high speed milling. CIRP Ann: Manuf Technol 1998;47(1): 307–10.
[6] Smith S, Dvorak D. Tool path strategies for high speed milling aluminum workpieces with thin webs. Mechatron J 1998;8(3):291–300.
[7] Arnaud L, Gonzalo O, Seguy S, Jauregi H, Peigné G. Simulation of low rigidity part machining applied to thin-walled structures. Int J Adv Manuf Technol 2011;54(5–8):479–88.
[8] Smith S, Wilhelm R, Dutterer B, Cherukuri H, Goel G. Sacrificial structure preforms for thin part machining. CIRP Ann: Manuf Technol 2012;61(1): 379–82.
[9] Smith S. Flexures: elements of elastic mechanisms. London, UK: CRC Press; 2000.
[10] Bae JS, Moon KK, Inman D. Vibration suppression of a cantilever beam using eddy current damper. J Sound Vib 2005;284:805–24.